

RADIATION PATTERN RETRIEVAL IN NON-ANECHOIC CHAMBERS USING THE MATRIX PENCIL ALGORITHM

G. León, S. Loredó, S. Zapatero, and F. Las Heras

Área de Teoría de la Señal y Comunicaciones
Departamento de Ingeniería Eléctrica
Universidad de Oviedo
Gijón 33204, Spain

Abstract—In this paper, the Matrix-Pencil method is used to retrieve the radiation pattern of several antennas measured in different semi-anechoic scenarios using low directive probes, where the existence of reflected contributions can severely disturb the measurement. Starting from data measured in the frequency domain, this method allows the direct path to be identified and the radiation pattern of the antenna to be retrieved with good accuracy in all the cases under study.

1. INTRODUCTION

Antenna radiation patterns are usually measured in anechoic chambers, where free-space conditions can be ensured. However, in any realistic measurement, imperfections appear: signal leakage from various sources and unwanted reflections and diffractions degrade the quality of the measurement. These unwanted effects are more important when low directive probes are used. Several techniques have been developed to overcome this lack of measurement quality. An analytical method for increasing the accuracy of the antenna measurements using a subtraction of spherical modes is studied in [1], whereas subtraction of plane waves is studied in [2]. A compensating method using equalizers is presented. The Matrix-Pencil (M-P) method is used in [3] to decompose a signal, measured in a semi-anechoic chamber, into a direct path and a reflected wave. This method and a FFT-based method for echo cancelation are compared in [4] by some of the authors of this paper.

Corresponding author: G. León (gleon@tsc.uniovi.es).

The M-P method [5] is an accurate algorithm for decomposing a complex signal into a sum of exponentials. This method has been successfully used in different topics, for example for location determination [6]. For our purpose, this method seems to be as accurate as the others, but it is preferable because it needs lower bandwidth than the FFT-based methods [4] and lower number of measurements than others. Therefore, the M-P method, particularly its total least squares version, has been chosen to retrieve the radiation pattern of different antennas measured in three semi-anechoic scenarios at different working bands using low directive probes, and some results are presented in this paper.

The paper is organized as follows. In Section 2, the three measurement scenarios and the M-P setup are described. In these scenarios, several pyramidal horn antennas and a monopole antenna were measured. The results of M-P application on measured data are presented in Section 3. Conclusions follow under Section 4.

2. MEASUREMENT SETUP

The measurements used in this experiment were carried out in the roll over azimuth spherical-range anechoic chamber ($8\text{ m} \times 5\text{ m} \times 4.5\text{ m}$) located in the ANTEM Lab at the University of Oviedo. Pyramidal horn antennas were used both as probe antennas and Antennas Under Test (AUT). A wideband planar monopole was also measured. The distance between the probe antenna and the AUT was 5.4 m .

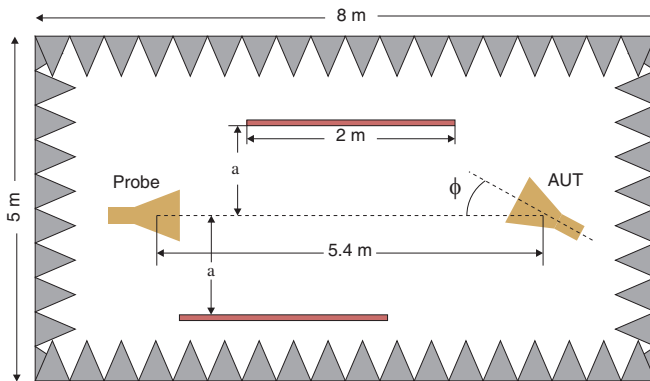


Figure 1. Top view scheme of the antenna-measurement experiment. One or two copper plates were introduced to achieve a reflected wave (scenarios 1 and 2) or two different reflected waves (scenario 3).

To achieve an undesirable reflection, one or two copper plates (with dimensions $2\text{ m} \times 1\text{ m}$) were introduced into the anechoic chamber between the probe antenna and the AUT. The scheme of the experiment can be seen in Fig. 1. The separations between the plates and the antennas' line of sight (parameters a and b) could be reconfigured, so that three different scenarios were studied: only one copper plate was present in scenario 1 and scenario 2, placed at a distance $a = 2.05\text{ m}$ and $a = 0.82\text{ m}$ respectively, while the second plate was also introduced to configure scenario 3. In this last scenario, the plates were placed at distances $a = 1.25\text{ m}$ and $b = 1.7\text{ m}$.

In order to validate the experiments, reference data of the transmission coefficient ($S_{21}^{ref}(\phi, f_0)$) were taken in anechoic environment, consisting of the azimuth (ϕ) radiation pattern of the AUT between 0° and 90° for an elevation angle (θ) equal to zero degrees, at different frequencies, and for all the antennas. For the monopole antenna, the elevation pattern was measured instead of the azimuth one.

The measurement campaign in the different non-anechoic scenarios was carried out in the frequency domain, measuring for each antenna the transmission coefficient $S_{21}^{mea}(\phi_i, f)$ of the system. The azimuth angle ϕ_i ranged from 0° to 90° in steps of 0.5° . For each angle, the transmission coefficient was sampled in a frequency bandwidth (BW) centered at a frequency f_0 with frequency step equal to Δf .

The measured data in the semi-anechoic chamber can be modeled as the sum of the direct path and the reflected waves [3]:

$$S_{21}^{model}(\phi_i, f) = \sum_{k=1}^M c_{ik} e^{\gamma_{ik} f} \quad (1)$$

where M is the number of waves to be considered in each scenario, that is, the number of complex exponentials used in the approach for each azimuth angle ϕ_i , c_{ik} is the complex amplitude for the k th complex exponential and $\gamma_{ik} = \alpha_{ik} + j\beta_{ik}$, being α_{ik} the damping factor that takes into account the attenuation due to propagation and the antenna factor, and β_{ik} a term directly related to the propagation time t_{ik} for each wave propagating through the whole measurement system (Equation (2) of [3]). The c_{ik} and γ_{ik} coefficients can be obtained applying the M-P algorithm to the set of measured samples ($S_{21}^{mea}(\phi, f)$) between $f_0 - BW/2$ and $f_0 + BW/2$, as explained in [4, 5]. In the M-P method, the number of waves M and the sampled bandwidth BW are parameters to fit. Previous works [4, 5] chose $M = 3$ for situations with only one strong reflection, using the third exponential term to give account of noise or other minor contributions. However, the M-P is a robust method against noise so this third term

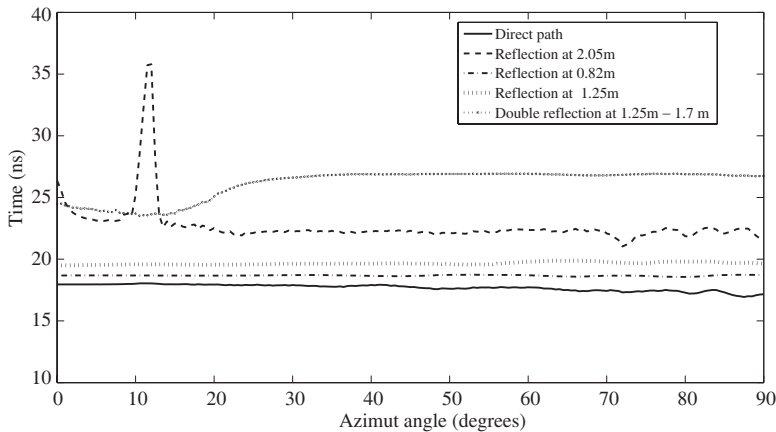


Figure 2. Delay time of the direct path and the reflected waves in different scenarios estimated with the M-P method for a pyramidal horn antenna at 10 GHz.

would not be really necessary. Several numerical simulations were performed in this work coming to the conclusion that when the number of exponential terms increases, also does the difficulty of identification of the different paths, which may result in larger differences between the retrieved and reference radiation patterns. Therefore, $M = 2$ was chosen for scenario 1 and 2, and $M = 3$ for scenario 3. In Figure 2, the delay time (t_{ik}) for the three different scenarios is plotted, when using pyramidal-horn antennas at $f_0 = 10$ GHz.

The direct path is identified as that with the exponential term with the lowest t_{ik} , and the radiation pattern without reflection can be retrieved as:

$$S_{21}^{ret}(\phi_i, f) = c_{id}e^{\gamma_{id}f} \quad (2)$$

where c_{id} and γ_{id} are the coefficients that model the direct path.

The soundness of the M-P method has been investigated in this work, varying the measured bandwidth and concluding that the results given by the M-P do not depend on the measured bandwidth whenever it ranges between $1/\delta t$ and $4/\delta t$, where δt is the time delay between the direct path and the first reflected wave. Outside this range, the accuracy of the method decreases.

The differences between the reference radiation pattern and the measured or the retrieved ones were estimated using respectively the

following error formulas:

$$E^{mea} = \frac{1}{N} \sum_{i=1}^N |\bar{S}_{21}^{ref}(\phi_i, f_0) - \bar{S}_{21}^{mea}(\phi_i, f_0)| \quad (3)$$

$$E^{ret} = \frac{1}{N} \sum_{i=1}^N |\bar{S}_{21}^{ref}(\phi_i, f_0) - \bar{S}_{21}^{ret}(\phi_i, f_0)| \quad (4)$$

where N is the number of measured angles, and \bar{S}_{21}^{ref} , \bar{S}_{21}^{mea} and \bar{S}_{21}^{ret} are respectively the normalized transmission parameters for the reference measurement, the measurement with reflection and the retrieved one for the i th azimuth angle at frequency f_0 . The normalization of each transmission parameter is relative to its maximum.

3. MEASUREMENTS AND RESULTS

Five different pyramidal-horn antennas were used as probes and AUTs in the first scenario under study, each of them at different frequencies and some of the results are presented next, corresponding to three different antennas and three different frequencies: 7.5 GHz, 10 GHz and 17 GHz. In this scenario, the estimated value for δt is 4.6 ns ($BW = 0.22$ GHz) and the maximum interference is expected around $\phi = 37^\circ$. The frequency step Δf is 1.25 MHz for the frequency band between 6 GHz and 8 GHz, and 2.50 MHz for the frequency sweeps 8.5 GHz–12 GHz and 16 GHz–18 GHz. In Figure 3 the reference,

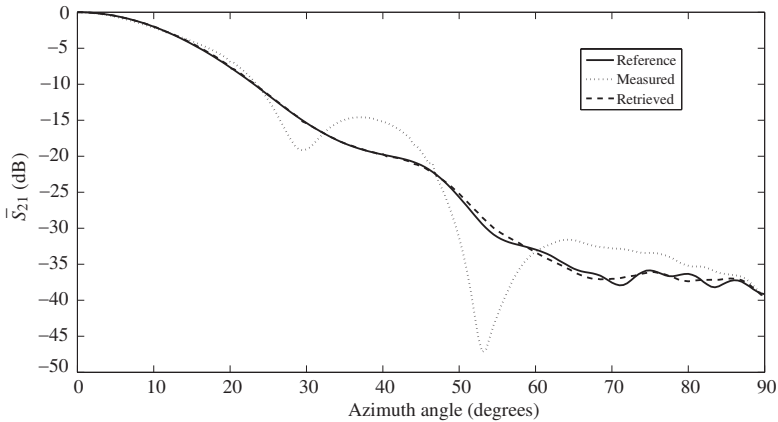


Figure 3. Reference, measured and retrieved radiation patterns of a pyramidal-horn antenna at 7.5 GHz in scenario 1.

measured and retrieved radiation patterns of a pyramidal-horn antenna at 7.5 GHz are plotted. It can be seen that the interference between the direct path and the reflected path begins around 20° , causing an initial error (E^{mea}) of 2.2%. The developed M-P algorithm retrieves the real radiation pattern of the antenna with good accuracy. Differences between both radiation patterns appear at angles above 65° , where the signal to noise ratio is very low. The recovery error is (E^{ret}) 0.19%.

Similar measurements were carried out with the two other antennas at 10 GHz (Fig. 4) and 17.5 GHz. In these cases, the interference between the two main paths begins at 15° , but because of the higher directivity at these frequencies the multipath power drops, causing an initial error of 2.2% and 1.2%, respectively. Good accuracy is also found, with recovery errors of 0.4% and 0.3%.

In scenario 2, the copper plate is located closer to the line of sight between the probe antenna and the AUT ($a = 0.82$ m). The estimated delay time for this configuration is 0.8 ns, therefore a wider frequency band was selected ($BW = 1.25$ GHz). A pyramidal antenna was measured in this scenario at frequency 10 GHz (Fig. 5) with $\Delta f = 2.50$ MHz. In this scenario, the influence of the copper plate can be appreciated in the whole radiation pattern, with a measured maximum at 28° and an initial error of 26.2%. The retrieved radiation pattern presents very good accuracy with the reference one, with a difference of 1.4%.

A more directive pyramidal antenna was also measured in scenario 2 at 20 GHz. The measured error was 1.3% and the recovery error was only 0.2%.

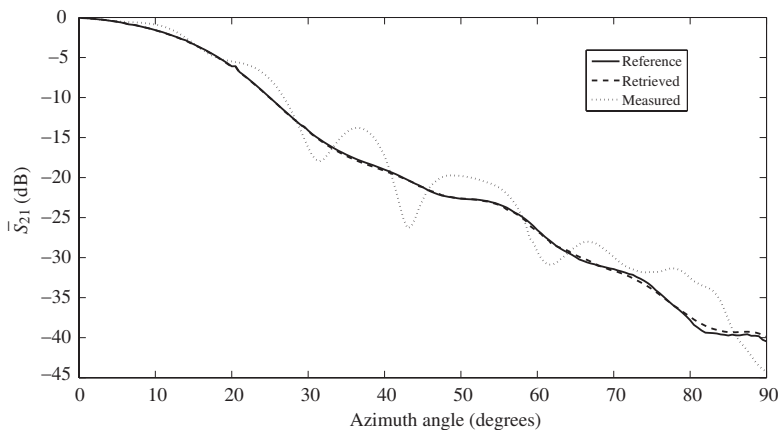


Figure 4. Reference, measured and retrieved radiation patterns of a pyramidal-horn antenna at 10 GHz in scenario 1.

A method based on FFT based method has also been applied to these measurements in order to retrieve the antenna radiation pattern [7], and it has been found that the magnitude of the recovery error is the same by both methods, but demanding the FFT-based method the double measured bandwidth.

A third scenario, with two copper plates, was configured to investigate the influence of a second reflection in the radiation pattern, and to prove the validity of the method in that situation. The second plate was located in such way that the double reflected path could

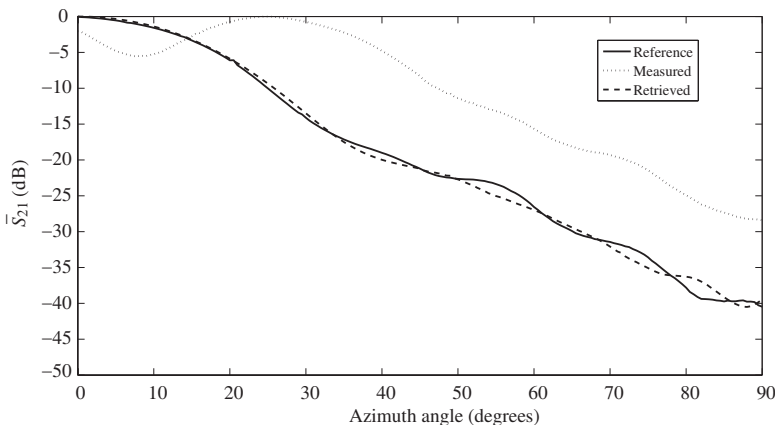


Figure 5. Reference, measured and retrieved radiation patterns of a pyramidal-horn antenna at 10 GHz in scenario 2.

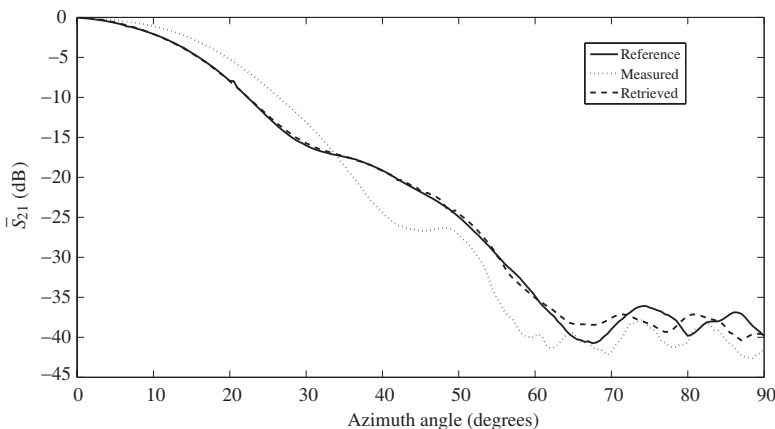


Figure 6. Reference, measured and retrieved radiation patterns of a pyramidal-horn antenna at 10 GHz in scenario 3 with $M = 3$.

reach out the probe antenna (Fig. 1). The delay time between the direct path and the first reflected path is $\delta t = 1.8$ ns. Again, a pyramidal horn antenna at 10 GHz was measured in these conditions (Fig. 6) and the measured error was 6.6%. A good agreement was found between the reference radiation pattern and those retrieved with the M-P method using $M=2$ (the double reflected contribution is low), $M=3$ and $M=4$. This proves again the soundness of the method. The best result appears using $M=3$, with a recovery error of 0.7%.

A wideband omnidirectional monopole antenna was also measured at 10 GHz in scenario 2 (Fig. 7). A directional pyramidal-horn was used as probe antenna. The differences between the reference radiation pattern and the measurement are greater than previous cases, and the measured error is 21.9%. The M-P method can retrieve the radiation pattern with good agreement, even when the elevation angle is 0° where only reflected radiation reaches the probe antenna. The retrieved error is 4.1%, because the error increases around 30° , where the influence of the copper plate is maximum. This antenna was also measured at 5 GHz and 7 GHz and similar results were found.

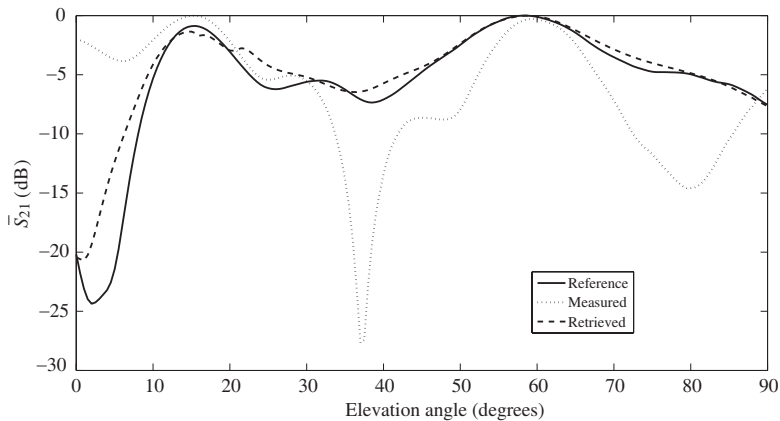


Figure 7. Reference, measured and retrieved radiation patterns of a wideband monopole antenna at 10 GHz in scenario 2.

4. CONCLUSION

The application of the Matrix-Pencil method to retrieve the radiation pattern of antennas measured in non anechoic conditions has been studied. The measurements in the frequency domain allow this method to model the received signal as a sum of exponential terms, one for the direct path and others for the reflected waves. With this method it

is possible to calculate the delay time of each path and to extract the direct path. Different pyramidal horn antennas and a monopole antenna were measured in three different scenarios, where one or two copper plates were located to ensure non-anechoic conditions. The M-P method was applied in all these cases and good accuracy was found between the retrieved radiation pattern and the reference one.

ACKNOWLEDGMENT

This work was supported by the “Ministerio de Ciencia e Innovación” of Spain under project TEC2008-01638/TEC (INVEMTA) and CONSOLIDER-INGENIO CSD2008-00068 (TERASENSE); and by the “Catedra Telefónica-Universidad de Oviedo”.

REFERENCES

1. Black, D. N. and E. B. Joy, “Test zone field compensation,” *IEEE Trans. Antennas Propagat.*, Vol. 43, No. 4, 362–368, 1995.
2. Leatherwood, D. A. and E. B. Joy, “Plane wave, pattern subtraction, range compensation,” *IEEE Trans. Antennas Propagat.*, Vol. 49, No. 12, 1843–1851, 2001.
3. Fouresti, B., Z. Altman, J. Wiart, and A. Azoulay, “On the use of the matrix pencil method to correlate measurements at different test sites,” *IEEE Trans. Antennas Propagat.*, Vol. 47, No. 10, 1569–1573, 1999.
4. Loredó, S., M. R. Pino, F. Las Heras, and T. K. Sarkar, “Echo identification and cancellation techniques for antenna measurements in non-anechoic test sites,” *Antennas Propagat. Mag.*, Vol. 46, No. 1, 100–107, 2004.
5. Hua, Y. and T. K. Sarkar, “Matrix pencil method for estimating parameters of exponentially damped/undamped sinusoids in noise,” *IEEE Trans. Acoust., Speech, Signal Processing*, Vol. 38, No. 5, 814–824, 1990.
6. Labib, A. L. and H. M. Elkarmouchi, “Location determination for 2G/3G/4G using time delay matrix pencil (TDMP) method,” *PIERS Proceedings*, 246–253, Hangzhou, China, March 24–28, 2008.
7. Loredó, S., G. Leon, S. Zapatero, and F. Las Heras, “Measurement of low-gain antennas in non-anechoic test sites through wideband channel characterization and echo cancellation,” *IEEE Antennas and Propagation Magazine*, Vol. 51, No. 1, February 2009.